Role of Insulation Materials and Cryogenic Coolants on Fault Performance of MW-Scale Fault-Tolerant Current-Limiting Superconducting Transformers

Mohammad Yazdani-Asrami, *Senior Member, IEEE*, Alireza Sadeghi, Seyyedmeysam Seyyedbarzegar, and Wenjuan Song, *Member, IEEE*

***Abstract*— Fault-Tolerant Current-Limiting (FTCL) High Temperature Superconducting (HTS) transformers are promising components for playing a role in renewable energy integrated modern power systems. In this paper, the impact of different insulation materials and cryogenic fluids on the electro-thermal characteristic of a MW-scale FTCL-HTS transformer is investigated. For this purpose, an Equivalent Circuit Model (ECM) is established to characterize the temperature, recovery time, and fault tolerability of FTCL-HTS transformer under different conditions. The proposed ECM is firstly validated using experimental results of a typical HTS transformer. After that the model is developed for a 50 MVA, 132 kV/13.8 kV HTS transformer. In order to add fault tolerance capability to the 50 MVA HTS transformer, three strategies were considered in this paper. In the first strategy, the effect of three insulation materials (including Kapton tapes, Nomex papers, and Acrylated Urethane solid insulation) covering HTS tapes was investigated on fault performance. The second strategy was changing cryogenic fluid to liquid hydrogen instead of liquid nitrogen. As for the last strategy, the impacts of thickness and material properties of stabilizer in HTS tape were investigated on the maximum temperature and recovery time of HTS transformer. Results show that by using these strategies, the maximum temperature of HTS tape of transformer winding under a short circuit fault was reduced.**

***Index Terms*— Electro-thermal behavior, Fault performance, high temperature superconducting transformer, solid insulation, protection, wind power system**

I. Introduction

High Temperature Superconducting (HTS) transformers are capable of carrying a much higher current in comparison to conventional oil-immersed transformers while their size is 45% lower than conventional transformers [1]. On the other hand, HTS transformers can operate indefinitely (if designed appropriately) under overloading condition without any thermal deterioration in their [1], [2]. These advantages of HTS transformers, along with their high efficiency and low risk of fire hazards, make them excellent choice for being used in electric power systems, especially those integrated with renewable energy resources such as wind [3], [4]. In power systems with high penetration level of wind renewable energy resources, the fault current level increases that could endanger the reliability, safety, and stability of the grid and its apparatuses. This is where Fault-Tolerant Current-Limiting (FTCL) HTS transformers offer a wide range of opportunities to improve fault performance and increase system stability. Currently in the wind farms conventional transformer together with conventional fault current limiter and breakers are used to limit and isolated a short circuit fault current, however, isolating the turbine cause reliability and system dynamic issues. The FTCL-HTS transformer is a very promising component to replace both conventional transformer and FCL to not only limit a fault but tolerating it without need to isolate the turbine from the system. As shown in Figure 1(a), in normal operation under steady state, the losses of conventional transformer and fault current limiter together is very high. If a fault occur, stability of the grid is at lowest possible value while the high impedance value of conventional transformer may lead to massive temperature increase of windings that could lead to burnout of

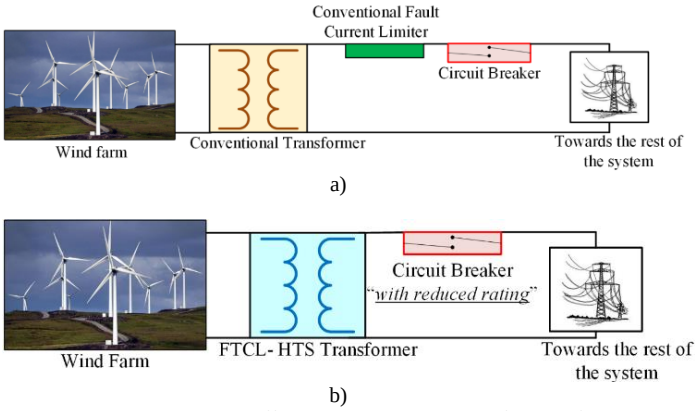

Figure 1. The opportunities offered by FTCL-HTS transformers facing with wind power integration

Manuscript received July 27, 2022, revised September 17 and October 14, 2022, accepted October 21, 2022.

M. Yazdani-Asrami and W. Song are with Propulsion, Electrification, & Superconductivity group, Autonomous Systems & Connectivity division, James Watt School of Engineering, University of Glasgow, Glasgow, G12 8QQ, United Kingdom. (Corresponding author's email: m.yazdaniasrami@gmail.com, mohammad.yazdani-asrami@glasgow.ac.uk)

A. Sadeghi and S. Seyyedbarzegar are with Department of Electrical Engineering, Shahrood University of Technology, Shahrood, Iran.

windings. However, conventional fault current limiter will reduce the level of fault current but it is very likely that wind turbine be isolated from network. On the other hand, there is a need for a high-power circuit breakers and conventional fault current limiter that could increase the total cost of the grid and increase the protection complexity of the grid. Thus, using FTCL-HTS transformers could help the engineers, designers, system operators, distribution/transmission companies, and other stakeholders of electric market to have a highly reliable and stable power grid connected to wind farms which operates at the lowest possible cost. It should be noted that by having grid structure of Figure 1(b), not only fault is limited and tolerated but also the load is supplied during fault that reduces the risk of load shedding and blackouts.

According to IEC 60076–5 standard, power transformers must be capable of tolerating short circuit faults for 2 seconds to increase the reliability, stability, and protection level of the power grid [5]. For conventional transformers with copper and aluminum windings, this can be easily achieved while for HTS transformers without any fault current limiting capability, a 2 second fault could rapidly increases the temperature of yttrium barium copper oxide (YBCO) tapes and causes the thermal runaway [5]. Thus, to avoid reliability issues and their voltage instability in power systems, there is a need for FTCL-HTS transformers. The FTCL-HTS transformers can operate under faulty conditions for a couple of seconds while the maximum temperature of YBCO tapes stays lower than thermal runaway threshold.

To reach to the concept of FTCL-HTS transformer, the main focus is on energy balance, i.e. the input energy in winding during fault would be dramatically increase, this will adiabatically increase the temperature of winding, since majority of this energy will store in thermal mass of coated conductor and in heat capacity of the stabilizer materials. The rest of energy should be transferred from superconductor to usually cooling fluid. One way to design a FTCL-HTS transformer is taking advantages of insulations that are mainly used for withstanding against electric field. By covering YBCO tapes with dielectrics, the heat transfer rate between the surface of the tapes and the cryogenic fluid is increased [5], [6]. This means that more heat is transferred to the cryogenic fluid and the temperature of the tape increases more slowly [6]. The second strategy is the use of Liquid Hydrogen (LH_2) instead of Liquid Nitrogen (LN_2). With respect to specific heat capacity and thermal conductivity of LH_2 in 20 K (the boiling temperature of LH_2), the temperature of YBCO tapes increase much less than the same fault under LN_2 cryogenic fluid. In addition, heat transfer of the fluid increases by reducing their temperatures [5], [6]. At last, by increasing the thermal mass of conductors, i.e. thicker superconductor tapes with thicker stabilizers, more energy can be stored in material and the rate of temperature increase of these tapes can be reduced and thus, thermal runaway is less likely.

In this paper, a 50 MVA, 132 kV/13.8 kV, fault tolerant current limiting HTS transformer is analyzed by using an Equivalent Circuit Model (ECM), implemented in MATLAB/SIMULINK. Firstly, the proposed ECM is validated by comparing the experimental results of a 45 kVA HTS transformer with the results of the simulations using ECM. After that the model is used for analyzing fault and recovery performance of a 50 MVA HTS transformer to make this transformer fault tolerant. To accomplish such a goal, three strategies are implemented, firstly, the effect of insulated HTS winding on fault and recovery performance of transformer is investigated, considering Kapton tape, Nomex paper insulation and Acrylated Urethane as solid insulation. Then, impact of type of cryogenic fluid and its operating temperature on heat transfer, and consequently fault tolerance of HTS transformer was investigated when coolant has changed from LN_2 to LH_2. At last, thermal mass of the YBCO tapes is increased to investigate the performance of HTS transformer. These three strategies are also shown in Figure 2. The performance of this 50 MVA FTCL-HTS transformer was analyzed then under different fault scenarios including different durations and also recovery under loads after fault clearance.

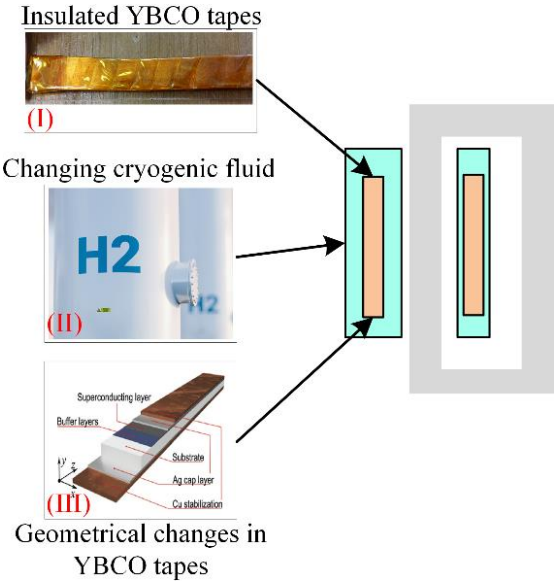

Figure 2. Three approaches for making a fault tolerant HTS transformer

II. MODELLING OF A FAULT-TOLERANT CURRENT-LIMITING TRANSFORMER

The aim of this section is to provide a guideline for the modelling procedure of a FTCL-HTS transformer. For this purpose, model formulations are divided into four subsections, electrical formulation, magnetic formulation, thermal formulation, and at last the procedure of applying these formulations in an ECM is discussed.

A. Electrical modelling of an HTS transformer

An ECM for an electric device is a combination of resistances, self and mutual inductances, and capacitances. Consider the HTS transformer shown in Figure 3. By using E-J power law of equation (1), the resistivity of YBCO tapes of the HTS transformer can be calculated, based on the variations of nominal current [7].

$$\rho_{YBCO} = \begin{cases} \rho_{ss} = \rho_0 & if\ J < J_c(T) \\ \rho_{ts1} = \rho_0 + \left(\frac{E_0}{J}\right)\left(\frac{J}{J_c(T)} - 1\right)^n & if\ J_c(T) < J < 3J_c(T) \\ \rho_{ts2} = \frac{\rho_{ts1} \times \rho_{sat}}{\rho_{ts1} + \rho_{sat}} & if\ J > 3J_c(T) \end{cases} \quad (1)$$

where, ρ_0 is the resistivity of YBCO tapes in steady state and considered to be $1 \times 10^{-14}\ \Omega.m$ [8], E_0 is 0.1 V/cm, J is current density, $J_c(T)$ is temperature dependent critical current density, n is index value of HTS tapes, and ρ_{sat} is the normal state resistivity of YBCO with a mean value of 90 $\mu\Omega\,.cm$ [8].

Equations (2) to (4) present the temperature and field dependency of critical current density and field dependency of index value, respectively [8]–[10].

$$J_c(T) = \begin{cases} J_c(T_b) & T < T_c \\ 0 & T > T_c \end{cases} \quad (2)$$

$$J_c(B_{per}, B_{par}) = \frac{J_c(0,0)}{\left[1 + \frac{\sqrt{(k_2 B_{par})^2 + (B_{per})^2}}{k_3}\right]^{k_1}} \quad (3)$$

$$n = n_0 \times \frac{B_1}{|B\ cos\ \theta| + B_1} \times \frac{B_2}{|B\ sin\ \theta| + B_2} \quad (4)$$

where, $J_c(T_b)$ is critical current density at base temperature T_b, T_c is critical temperature, n_0 is considered to be 25, B is magnetic field density, B_1 and B_2 are considered to be 2 T and 1 T respectively, θ is field angle, B_{par} is the parallel component of magnetic field, B_{per} is the perpendicular component of magnetic field, k_1, k_2, and k_3 are considered to be 0.758, 0.0605, and 103 [8]–[10].

The YBCO coated conductor tapes consist of different materials such as copper, silver, and insulation. To calculate their resistances, the well-known resistivity-temperature formulation of equation (5) is used.

$$\rho_{mat}(T) = \rho_{R-mat}[1 + \alpha_R(T - T_b)] \quad (5)$$

where, $\rho_{mat}(T)$ is the specific resistivity of material in temperature T, ρ_{R-mat} is the specific resistivity of material in base temperature, and α_R is the temperature coefficient of the resistivity.

After calculation of resistivity, self and mutual inductances must be calculated for each winding of transformer. The self- and mutual inductances are calculated based on equations (6) and (7) [11], [12].

$$L_i = \frac{N_i^2 \mu_0 \mu_r A_{fp}}{\ell} \quad (6)$$

$$M_{ij} = \frac{N_i N_j \lambda_i}{I_j} \quad (7)$$

where, N is turn number, μ_0 is permeability of free space equal to $4\pi \times 10^{-7}$ H/m, μ_r is relative permeability of the core material, A_{fp} is the cross-sectional area of the flux path, ℓ is the stack height of the windings, λ_i is the flux linkage of layer i, and I_j is the excitation current of winding j.

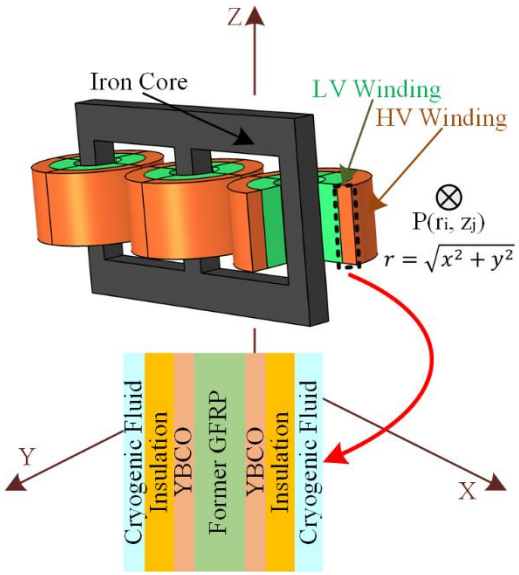

Figure 3. Schematic of a typical 3-phase HTS transformer. The GFRP stands for Glass Fiber Reinforced Plastic.

B. Magnetic modelling of an HTS transformer

Magnetic flux density in the transformer is time-dependent and it varies along with respect to the height of superconducting windings, the nominal current of transformer, and the properties of the core. Axial and radial magnetic flux densities are expressed in equations (8) and (9) [13], [14]:

$$B_{ax} = \sqrt{2}\frac{\mu_0 I_t N}{\ell_c}\beta \quad (8)$$

$$B_r = \sqrt{2}\frac{\mu_0 I_t N}{\ell_c}\alpha \quad (9)$$

where, I_t is the RMS current passing through the HTS windings and ℓ_c is the half of the coil height, here $h_{coil} = [-\ell_c\ \ell_c]$ and $\ell_c = \frac{h_{coil}}{2}$. If we consider the point (r_i, z_j) of field calculation as $P(r_i, z_j)$, then, we have equations (10) and (11) for α and β [13], [14]:

$$\beta = \frac{1}{2\pi}\left|\tan^{-1}\frac{\frac{2z_j}{\ell} + 1}{\frac{2r_i}{\ell}} - \tan^{-1}\frac{\frac{2z_j}{\ell} - 1}{\frac{2r_i}{\ell}}\right| \quad (10)$$

$$\alpha = \frac{1}{4\pi}\left[\ln\frac{\left(\frac{2r_i}{\ell}\right)^2 + \left(\frac{2z_j}{\ell} - 1\right)^2}{\left(\frac{2r_i}{\ell}\right)^2 + \left(\frac{2z_j}{\ell} + 1\right)^2}\right] \quad (11)$$

At last perpendicular and parallel magnetic field can be calculated with respect to the twisting angle of HTS tapes around the former (θ_f), as expressed in equations (12) and (13) [13], [14]:

$$B_{par} = B_{ax}\cos(\theta_f) + B_r \sin(\theta_f) \quad (12)$$

$$B_{per} = B_{ax}\sin(\theta_f) + B_r \cos(\theta_f) \quad (13)$$

By knowing the values of the magnetic field, total loss in transformer could be calculated using equation (14) [15]:

$$P_{total} = P_{fe} + C_{pen}(P_{sf} + P_{par} + P_{per} + P_{cl} + P_{cr}) \quad (14)$$

where, P_{fe} is iron-core loss, P_{sf} is self-field loss, P_{par} is parallel field loss, P_{per} is perpendicular field loss, P_{cl} is current lead loss, P_{cr} is cryostat loss, and C_{pen} is cooling penalty factor which is considered as 18 at operating temperature of 65 K.

Loss components are expressed in equations (15) to (20) [15].

$$P_{sf} = \frac{f I_c^2 \mu_0}{\pi}\left[\left(1-\frac{I}{I_c}\right)\ln\left(1-\frac{I}{I_c}\right)+\left(\frac{I}{I_c}-\frac{I^2}{2I_c^2}\right)\right] \quad (15)$$

$$P_{par} = \begin{cases} \frac{2fCA_c}{3\mu_0 B_P} B_{par}^3 & B_{par} < B_P \\ \frac{2fCA_c B_P}{3\mu_0}(3B_{par} - 2B_P) & B_{par} > B_P \end{cases} \quad (16)$$

$$P_{per} = Kf\frac{w^2\pi}{\mu_0} B_c B_{per}\left[\frac{2B_c}{B_{per}}\ln\left(\cosh\frac{B_{per}}{B_c}\right) - tanh\frac{B_{per}}{B_c}\right] \quad (17)$$

$$P_{cl} = 6q_{cl}(I_{LV} + I_{HV}) \quad (18)$$

$$P_{cr} = \frac{\lambda_{th}}{th_{ins}} A_{cr}\Delta T \quad (19)$$

$$P_{fe} = 1.2 c_p G_{fe} \quad (20)$$

where, f is frequency, I_c is critical current, C is ratio between the superconductor cross section and the total tape cross section, B_P is the full penetration flux density, A_c is the total tape cross section, B_c is the critical field, K is geometrical parameter, w is the tape width, q_{cl} is the specific thermal income per unit current and considered to be 45 kW/kA [15], I_{LV} is current at low voltage side, I_{HV} is the current at high voltage side (in kA), λ_{th} is thermal conductivity of cryostat, th_{ins} is the thermal insulation thickness, A_{cr} is the cryostat surface, G_{fe} is the weight of the core, and c_p is the loss per unit weight of ferromagnetic material that is considered to be 1.4 W/kg [15].

When HTS transformer is firstly energized, a massive current would be drawn from the power network known as the inrush current [16]. This current is a massive current similar to fault and its impact on transformer must be studied. To model inrush current, firstly, saturation reactance of core must be calculated according to equation (21) [17]:

$$X_s = \frac{2\,\mu_0\, N^2\, A_{mtw}\ \pi\, f}{Z_w} \quad (21)$$

where, N is the number of turns in energized winding (here is low voltage (LV) side), A_{mtw} is the mean area of energized winding, and Z_w is the height of the same winding. After that, the angle of core saturation instance (ξ_c) is calculated as equation (21) [16]:

$$\xi_c = \cos^{-1}\frac{(B_{sat} - B_m - B_{residual})}{B_m} \quad (22)$$

where, B_{sat} is saturation flux density, $B_{residual}$ is residual flux density, and B_m is the peak flux density of core. At last, in an iterative process, inrush current and residual flux density are calculated until the full suppression of inrush current, based on equations (23) and (24) [17]:

$$I_{inrush_{peak}} = \frac{1.6263 \times V\,(1-\cos\xi_c)}{X_s} \quad (23)$$

$$B^{t_{i+\Delta t}}{}_{residual} = B^{t_i}_{residual} - \left[\frac{2.26 \times B_{max}\, R_w}{X_s}(2 \times (\sin\xi_c - \xi_c\cos\xi_c))\right] \quad (24)$$

where, V is voltage, t is time, B_{max} is maximum value of designed steady-state flux density in the core, and R_w is average resistivity of winding.

C. Thermal modelling of an HTS transformer

Equation (25) is used to describes the heat transfer in cryogenic environment in HTS transformer [18]–[20].

$$D(T)C_p(T)\frac{\partial T}{\partial t} = \lambda(T)\frac{\partial^2 T}{\partial x^2} + Q - \nabla q \quad (25)$$

where, $D(T)$ is the density of the material (kg/m^3), $C_p(T)$ is specific heat capacity (J/kg.K), $\lambda(T)$ is thermal conductivity of material (W/m.K), Q is generated/transferred heat (W/m^3), and ∇q is heat flux (W/m^3). It should be noted that ∇q is the flow of energy per unit area while the Q is the amount of energy generated/transferred in superconducting windings. Equation (25) is valid for the superconducting layer and the insulations covering the HTS tapes. Q have different values for YBCO and dielectric layers in different operating states. Table 1 shows the information about the Q values in different states. In this table, Q_{AC} is the heat from AC loss; Q_J is heat from Joule loss; Q_{y2d} is the conduction heat transfer from superconductor to dielectric; and Q_{y2c} is the convective heat transfer from dielectric to coolant fluid [21].

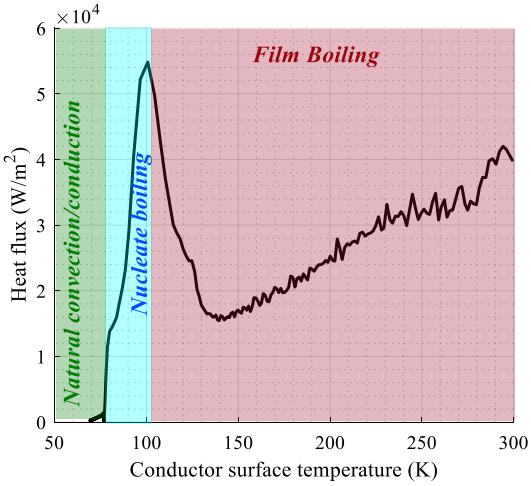

Figure 4. Heat transfer regime in LN_2 (W/m^2) per cross-section area of HTS tape

Table 1. The generated/transferred heat (W/m^3) for superconductor and dielectric materials during different operating states of HTS transformer

	Superconductor	Dielectric
Steady state	$Q = Q_{AC} - 2Q_{y2d}$	$Q = 2Q_{y2d}$
Transient state	$Q = Q_J - 2Q_{y2d}$	$Q = 2Q_{y2d}$
Recovery state	$Q = Q_J - 2Q_{y2d}$	$Q = 2Q_{y2d} - 2Q_{y2c}$

Heat flux is required to accurately solve the equation (22). However, heat flux value changes at different heat transfer regimes. Figure 4 illustrates the heat transfer regimes in LN2 that is classified under three modes, natural convection/conduction, nucleate boiling, and film boiling [5], [6], [18]. According to Figure 4, for temperatures near the base temperature which is the case in steady state operation of HTS transformers, heat flux is small and a little heat is transferred to the LN_2. This is the case when a little heat transfer is enough for dissipating AC loss from winding under steady state condition. When the conductor temperature starts to increase, heat flux increases also until a heat transfer peak where critical heat flux is appeared. Under this regime, LN_2 starts to be vaporized in a form of bubbles and a massive amount of heat is transferred to the cryogenic fluid. Under such circumstances, gas bubbles remove the heat from the surface of coated conductor tape and therefore, temperature increase rate is reduced. If surface temperature keeps increasing, bubbles form a thick layer of gas sheath on the surface of conductor in film boiling regime, and this results in a drastic heat transfer reduction and thus the temperature increases much faster which will lead to thermal runaway if no appropriate solution is considered and implemented. More information regarding heat transfer regimes in HTS transformers could be found in [5], [6].

Equations (26) to (30) were derived from heat transfer experiments in [5], [6], [22] to present the heat flux values for different operating conditions and regimes.

$$q_{bare-LN_2} = \begin{cases} -285.6\,T + 2.359\times10^4 & T < 80 \\ -100.1\,T^2 - 1.942\times10^4 T - 9.136\times10^5 & 80 \le T < 113 \\ 0.4444\,T^2 - 58.74T + 90.84 & T \ge 100 \end{cases} \quad (26)$$

$$q_{bare-LH_2} = \begin{cases} 100\,(T-20)^{6.3} & T < 23 \\ 10^5 (T-20) & 23 \le T < 120 \\ 1000(T-20) & T \ge 120 \end{cases} \quad (27)$$

$$q_{Nom-LN_2} = \begin{cases} -507\,T + -3.517\times10^4 & T < 83 \\ -48.44\,T^2 + 1.105\times10^4 T - 5.621\times10^5 & 83 \le T < 113 \\ 1.667\,T^2 - 658.9T + 8.959\times10^4 & T \ge 100 \end{cases} \quad (28)$$

$$q_{Kap-LN_2} = \begin{cases} 257.9\,T + -1.799\times10^4 & T < 83 \\ -131.9\,T^2 + 2.669\times10^4 T - 1.3\times10^6 & 83 \le T < 113 \\ 0.6588\,T^2 - 146.1T + 2.668\times10^4 & T \ge 100 \end{cases} \quad (29)$$

$$q_{\mathrm{Acry}-LN_2} = \begin{cases} 365.1\,T - 2.814\times10^4 & T < 78 \\ -225.7\,T^2 + 4.182\times10^4 T - 1.799\times10^6 & 78 \le T < 113 \\ -4.456T^2 + 1987T - 9.788\times10^4 & T \ge 100 \end{cases} \quad (30)$$

where $q_{bare-LN_2}$ is heat flux of bare tape in LN_2, $q_{bare-LH_2}$ is the heat flux of bare tape in LH_2, q_{Nom-LN_2} is the heat flux of insulated tapes by Nomex papers, q_{Kap-LN_2} is the heat flux of insulated tapes by Kapton papers, and $q_{\mathrm{Acry}-LN_2}$ is the heat flux of insulated tapes by Acrylated Urethane solid insulation. All heat fluxes must be divided to height of HTS coil to have these values in (W/m^3).

D. Electromagnetic coupled with thermal model

Figure 5(a) shows the implementation procedure of the proposed ECM. According to this figure, after gaining the geometrical parameters of the HTS transformer, the model can be built with resistances, capacitances, and inductances. The ECM for HTS transformer is shown in Figure 5(b). In this figure, subscript "p" and "s" are devoted to primary and secondary side of transformer, respectively. At last, the sectioned ladder model of HTS windings is used for the analysis in this paper, as shown in Figure 5(c). For having a more accurate transient model, the sections are selected to be 1000 [23]. In Figure 5(c), $R_{ins\text{-}top}$ and $R_{ins\text{-}down}$ are referred to resistivity of different insulations, R_{cu} is resistivity of stabilizer, R_{ag} is resistivity of shield layer of tape, R_{sc} is variable resistivity of superconducting layer, and R_{hsat} is resistivity of substrate layer. A parallel link between MATLAB coding environment and SIMULINK is established to update the values of resistances and inductances of the HTS tapes according to procedure shown in the flowchart of Figure 6. If flowing current exceeds the critical current, the HTS transformer windings will go out of superconducting mode. Thus, the temperature rises, resistance, and other electrothermal properties are updated and the values of resistance, inductance, and capacitances are updated for the next iteration. On the other hand, if the current is lower than the critical value, the temperature determines the operating state of the HTS transformer. If temperature exceeds the critical temperature value, the HTS transformer is in recovery regime, otherwise the transformer is in steady state (natural convection/conduction regime of heat transfer). In both states, the parameters of ECM are updated and then prepared for the next iteration. At last, the time interval is updated and checked if meeting the stopping criteria.

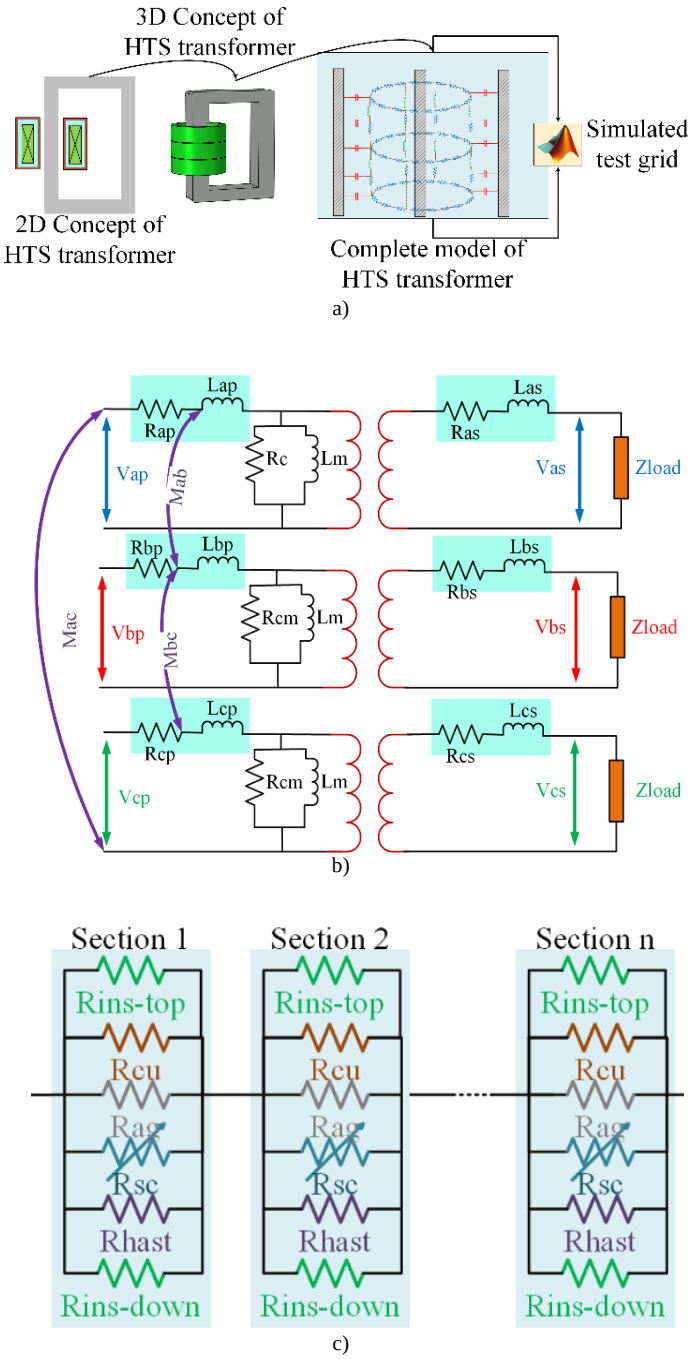

Figure 5. The model of FCLT-HTS transformer, a) ECM concept, b) ECM of HTS transformer in MATLAB-SIMULINK, and c) sectioned ladder model of HTS windings

III. Model Validation by Experimental Results

Before any further analysis, firstly, the proposed ECM must be validated. Thus, the proposed model was used to simulate winding temperature of a 45 kVA HTS transformer under a 0.33 seconds fault while two recovery under load scenarios are considered, i.e. 20% and 140% of loading after fault clearance. It should be noted that the HTS windings are covered by Acrylated Urethane solid insulation to increase heat transfer. Table 2 tabulates the most important parameters of the 45 kVA transformer, reported in [6].

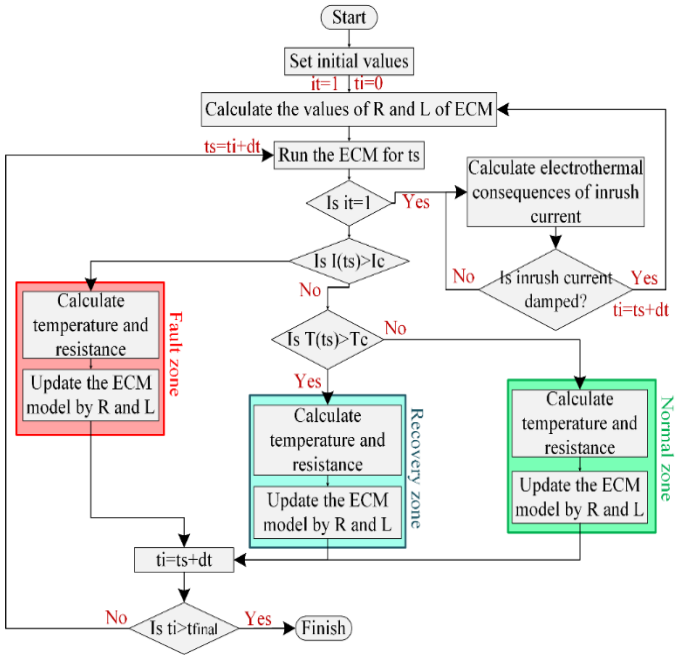

Figure 6. Modelling flowchart of the FCLT-HTS transformer using ECM

TABLE 2. The specifications of the 45 kVA HTS transformer, used for validation of the proposed ECM

Parameter	Value	Unit
Voltage V_1 and V_2	0.45	kV
Current I_1 and I_2	100	A
Turn number N_1 and N_2	38	-
Base temperature	65	K
Base impedance	4.5	Ω
Layer number	1	-

The results of validation are shown in Figure 7(a) and Figure 7(b) for 20% and 140% post-fault loading. It should be mentioned that the faults were imposed to the secondary side of 45 kVA HTS transformer. As depicted in Figure 6, the experimental data and simulation results are in a good agreement with each other. However, the rate of experimental temperature increase is a bit slower than the result of simulations. This is due to the fact that simulations are conducted based on a completely adiabatic environment during transients while in real world, a very small fraction of generated heat is transferred to the winding former, insulations, and coolant. As shown in Figure 7, the proposed ECM has a high accuracy in modelling the electro-thermal characteristic of the HTS transformer and therefore, this validated ECM could be used for other studies in the following sections.

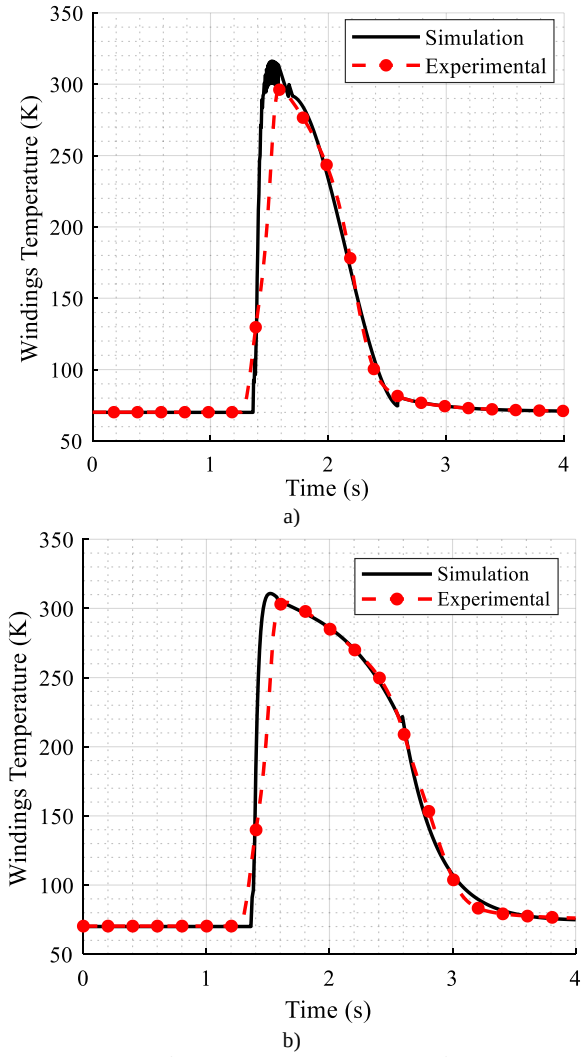

Figure 7. Validation of the proposed ECM, tested for a 45 kVA HTS transformer, a) time dependency of temperature for recovery under load of HTS transformer when 20% of load is applied after fault clearance, b) time dependency of temperature for recovery under load of HTS transformer when 140% of load is applied after fault clearance

Table 3. The general specifications of the understudied HTS transformer identical for both primary and secondary sides

Parameter	Value/type	Unit
Apparent power	50	MVA
Cryogenic fluid	LN_2	Subcooled
Basic Insulation Level (BIL)	550	kV
Operational temperature	65	K
Frequency	60	Hz
Maximum flux density in core	1.6	T
Total leakage reactance	0.067	p.u.
Magnetization reactance	105	p.u.

Table 4. The specifications of 50 MVA HTS transformer at primary and secondary sides

Parameter	Primary side	Secondary side	Unit
Nominal voltage	132	13.8	kV
Number of strands	8	17	-
Nominal current	480	2250	A
Number of turns	860	156	-
Number of layers	10	4	-
Clearance between layers	0.05	0.025	mm
Turns per layer	86	39	-

Table 5. The specifications of YBCO tape, used in 50 MVA HTS transformer

Layer	**Material**	**Thickness (μm)**
Stabilizer	Copper	40
Shield	Silver	3.8
Substrate	Hastelloy	50
Superconducting	YBCO	1

A. Case study: 50 MVA fault-tolerant current-limiting HTS transformer

To analyze the impact of different strategies on fault tolerability of HTS transformers, a 50 MVA, 132 kV/13.8 kV, 60 Hz, 65 K transformer is modeled. It is due to the fact that the breakeven power for HTS transformer technology is above 20 MVA [14]. Manufacturing the HTS transformers in MW-scale at 77 K temperature of saturated vapor pressure (SVP) LN_2 is not realistic and these transformers must be designed for operating at 65 K with subcooled LN_2. This is because of the high AC loss, low heat transfer, and high boil-off rate at SVP 77 K comparing to subcooled 65 K. Therefore, the understudied HTS transformer is considered to operate at 65 K subcooled LN_2.

More details regarding design procedure of this 50 MVA HTS transformer can be found in [24]. Second generation YBCO HTS tapes are used as the conductors in windings of this transformer. The main parameters of the understudied transformer are tabulated in Table 3 while some specifications of the primary and secondary windings are shown in Table 4. Table 5 also shows the most important geometrical specifications of the sub-layers in 4.4 mm width and 100 μm thick YBCO tape used in the 50 MVA HTS transformer. According to [24], total critical current of primary windings is about 530 A while this value for secondary windings are 2550 A.

As shown in Figure 8, this 50 MVA HTS transformer is used as step-down transformer to connect a 132 kV transmission line system to a substation with 13.8 kV voltage for supplying50 MVA load to load center. A three-phase fault is imposed to the grid with a 500 ms duration. Figure 9 shows the imposed fault current to the LV side of the HTS transformer. The maximum value of fault current is about 20 times higher than nominal current of HTS transformer. As can be seen from Figure 9, the fault causes a temperature peak of 450 K, and therefore, the burnout of HTS tapes is almost certain as maximum tolerable temperature of the YBCO superconductor is about 400-500 K.

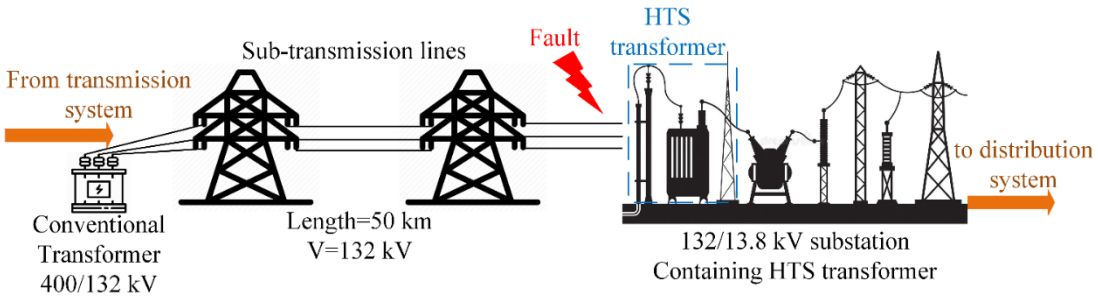

Figure 8. Test grid of the 50 MVA HTS transformer

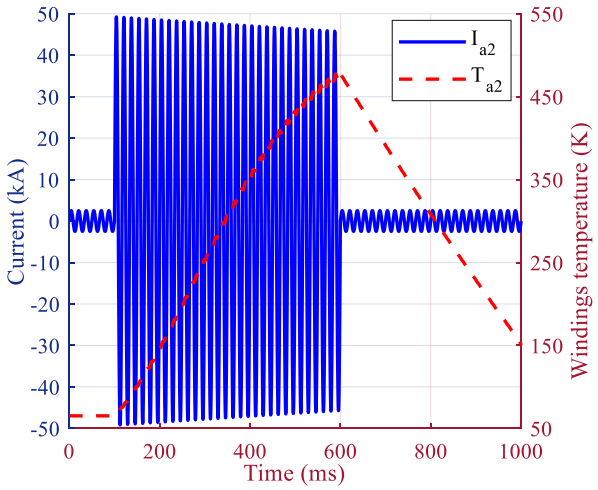

Figure 9. The electrothermal characteristic of the 50 MVA HTS transformer with bare tapes under a 500 ms three-phase fault

Therefore, to protect the HTS transformer and other components in substation, it should be isolated from the network using relay protection system. Fast circuit breakers should be implemented in the substation to isolate the HTS transformer under the fault well-before temperature reaches to dangerous margin. If HTS transformer is isolated, the supply of demanded load/power to load center during and after transient state would be disrupted. These consequences are due to the fact that temperature of superconducting winding surpasses the threshold value of 400 K. Thus, in rest of the paper we offer a solution to add fault tolerance capability to the proposed 50 MVA HTS transformer.

B. Insulation characteristics as a solution towards the FTCL-HTS transformer

To have a FTCL-HTS transformer, transformer needs to tolerate a fault for longer time when operating safely well-below burnout temperature of the superconducting tapes in windings. To do so, one way is to transfer more heat during the fault to the cryogenic coolant. To dissipate more heat from the surface of superconductors in transformer winding during a course of fault, one way is by extending nucleate boiling regime as it has the highest heat flux, but to keep away from film boiling. So, to keep the gas sheath away during a fault, the tapes should be insulated [5], [6].

In this paper, three insulation materials are considered, Aramid paper, i.e. Nomex, Polyimide paper, i.e. Kapton tape, and a solid insulation i.e. Acrylated Urethane. The logic behind this selection is the fact that even though Kapton tape is the most common insulation material for superconducting application, it is not a good option for HV applications and it is thermally very vulnerable at high temperatures. Although Nomex is a common insulation for manufacturing HV conventional transformer, the cooling fluid might penetrate underneath it and during a fault by establishing gas sheath reduces heat transfer and cause thermal runaway. At last, Acrylated Urethane which is very common insulation in automotive and aerospace industries, is a good insulation for HV applications and in addition, cooling fluid cannot penetrate underneath it as this solid insulation totally cover the tape [25]. In this analysis the thickness of the insulation layers is varied from 20 µm to 140 µm. This is conducted to help the readers to understand the impact of insulation thickness on the electrothermal behavior of the HTS transformer. In addition, for modelling heat transfer for these three insulation materials, experimental heat flux specification shown in equations (25) to (29) were considered and implemented. At last, it should be mentioned that in the current study, not only time-dependent characteristic of temperature is considered but also the temperature profile of winding layers in radial distance is considered. Figure 10 shows the transient temperature profile for HTS windings with three different insulation materials along the radial distance. Every temperature reported in this paper, is the peak value in radial direction.

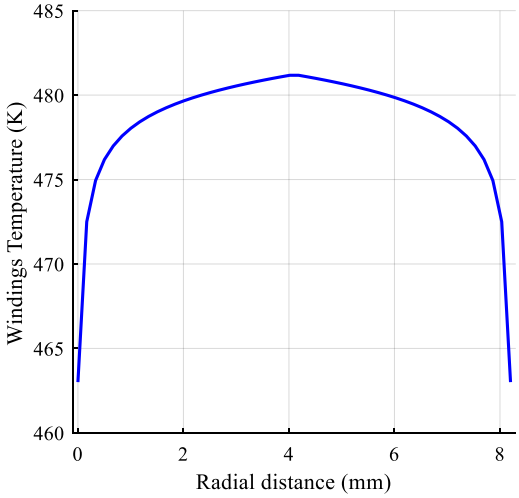

a) Bare tape

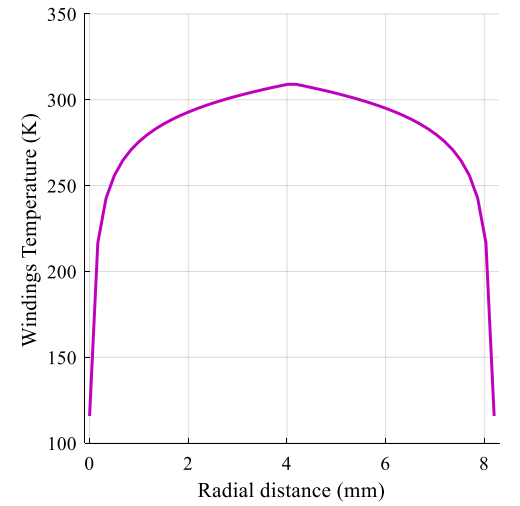

b) Kapton insulated

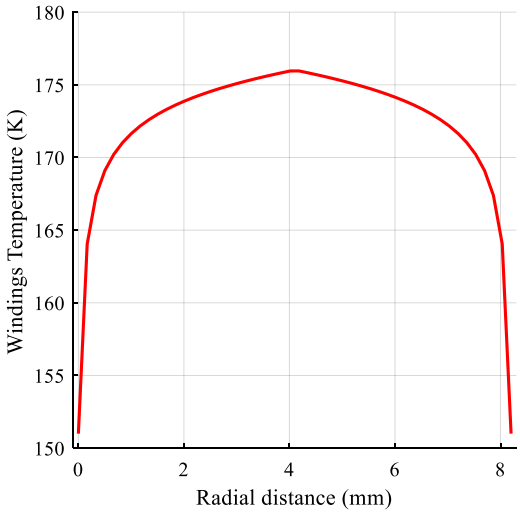

c) Nomex insulated

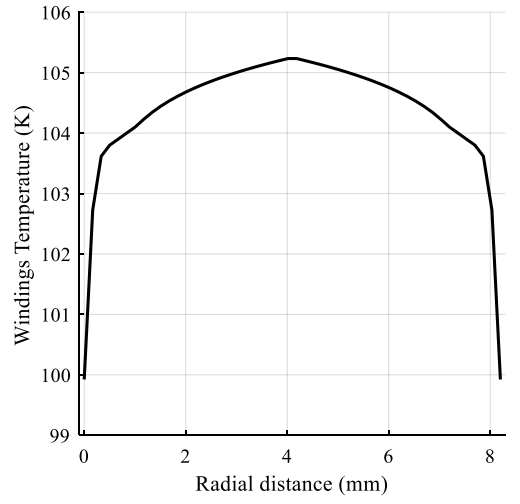

d) Acrylated Urethane solid insulated

Figure 10. Temperature profile of HTS transformer in radial distance

Figure 11(a) shows the maximum temperature of the HTS tapes in secondary winding of the phase A of HTS transformer, when tapes are covered by Kapton tapes. It is obvious that using Kapton reduces the peak temperature compared with bare tape, from 500 K to 400 K. The thinner the insulation gets, the value of maximum temperature is reduced. The HTS winding covered by Kapton tape will be at lower risk of reaching burnout temperatures, however, reaching and staying at temperatures higher than 300 K (room temperature) will dramatically increase the chance of establishing and initiating hotspot in HTS winding of transformer locally. The thermal performance of the HTS winding insulated with Nomex paper is also shown in Figure 11(b). Maximum temperature of winding reduces by about 50 K, which will also reduce the risk of hotspot in the windings. As can be seen the thermal performance of the Nomex paper outweighs the Kapton tape. This is due to higher heat transfer, and better thermal properties of Nomex paper such as heat capacity and thermal conductivity. The best thermal performance is observed when conductor surface is covered by Acrylated Urethane solid insulation as shown in Figure 11(c). The maximum temperature reaches to about 120 K after a 2 s fault which is halved compared with when winding is insulated by Nomex paper. This means that the HTS transformer is capable of tolerating fault current for 2s without any possibility of burnout. This is due to much higher heat transfer and heat flux that of the solid insulation offers.

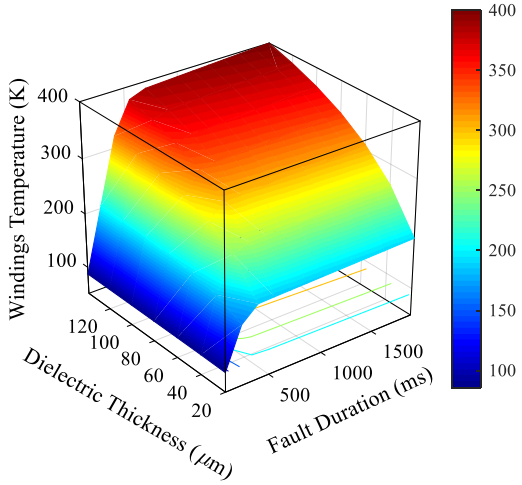

a) Kapton insulated

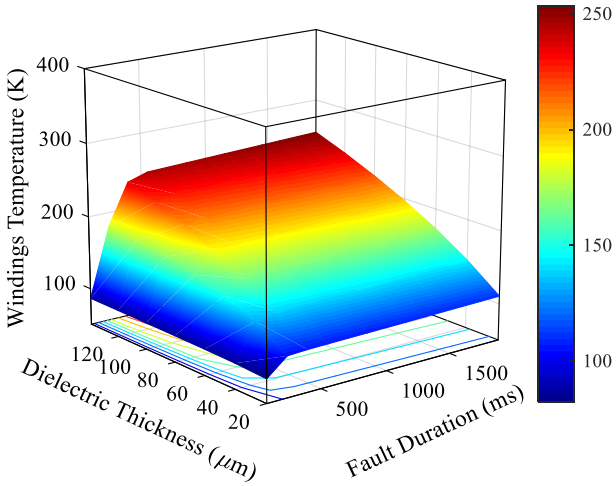

b) Nomex insulated

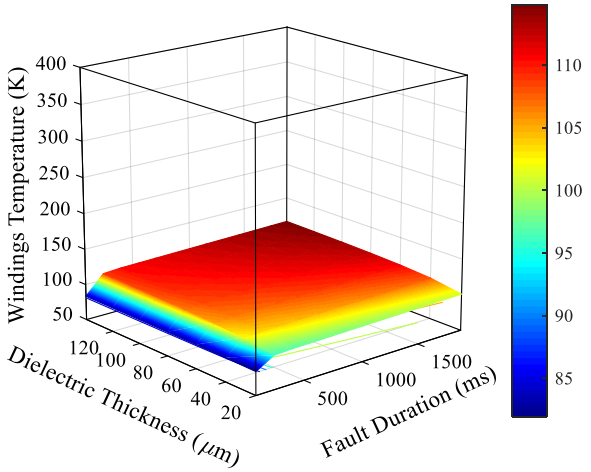

c) Acrylated Urethane solid insulated

Figure 11. Time dependency of temperature of secondary winding of 50 MVA HTS transformer when tapes are covered by different insulations: a) Kapton tape. b) Nomex paper. c) Acrylated Urethane solid insulation

The reason behind this fascinating performance is due to this fact that the surface of insulation is cooler than surface of bare conductor, therefore, when coolant touches the surface does not quickly evaporate to produce gas sheath around conductor. This means that by using Acrylated Urethane, the film boiling regime requires a longer time to take place and as a result of this the value of maximum temperature would be reduced. Therefore, if HTS transformer winding is covered by Acrylated Urethane solid insulation, the 2 seconds fault withstanding requirement of IEC 60076–5 standard would be satisfied, and FTCL-HTS transformer concept would be achieved.

1) Recovery under load of the FTCL-HTS transformer

In this subsection, the impact of recovery under load after fault clearance is discussed. Recovery under load is critical for increasing the reliability of power network. Firstly, the discussion is made on HTS transformer with bare tapes. As can be seen in Figure 12(a), under a 500 ms fault and for any load higher than 50% of rated load, the temperature of winding surpasses the maximum tolerable temperature of YBCO tapes and thus, windings suffer burnouts. On the other hand, the maximum loading in which HTS winding can be recovered without experiencing any thermal runaway, is 55% of nominal load. Figure 12(b) illustrates the impact of covering the YBCO tapes by a 70 μm thick Kapton tape. As can be seen, the maximum temperature under full load is 50% reduced by using Kapton tape compared with bare conductor. However, under 100% and 75% loading, HTS transformer is not recoverable to superconducting state and still faces a thermal runaway. Also, the maximum recoverable loading for HTS transformer 9.1% increases and becomes around 60% of rated load. To make more improvements, according to Figure 12(c), 70 μm thick Nomex paper was also tested and the transformer winding covered by Nomex papers, could recover under 50% of nominal loading. Also, by changing the insulations to Nomex paper, the maximum loading of HTS transformer under recovery increases and becomes 65%. At last, when the solid insulation is used, the HTS transformer is fully recoverable under full rated load.

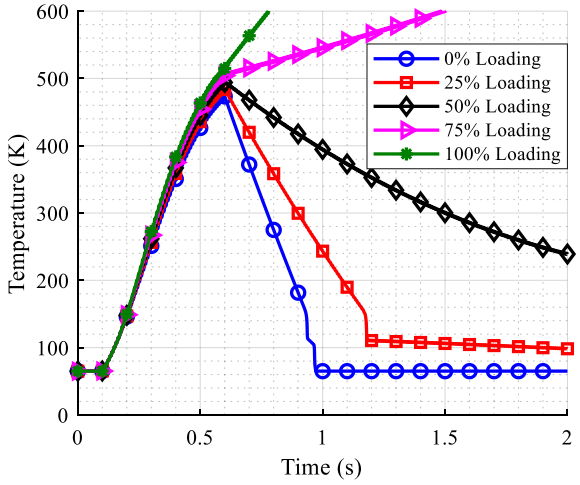

a) Bare tape

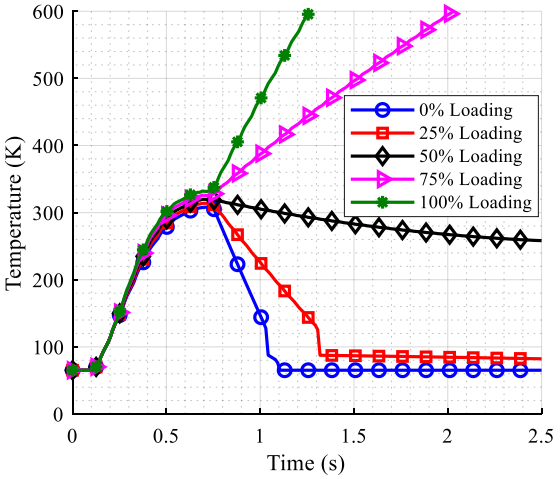

b) Kapton insulated

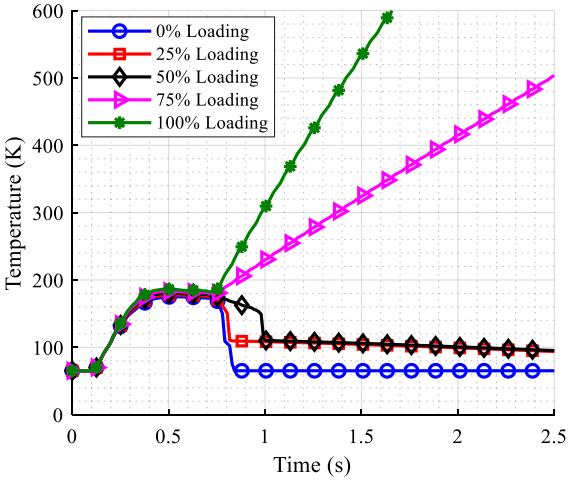

c) Nomex insulated

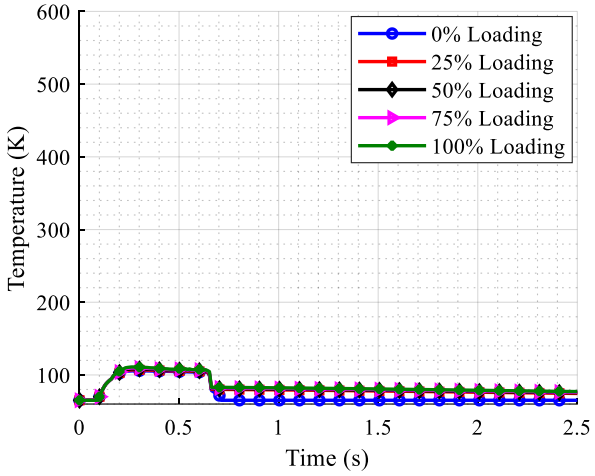

d) Acrylated Urethane solid insulated

Figure 12. Recovery under load of 50 MVA HTS transformer under different loading conditions and insulations for 500 ms fault

As shown in Figure 12(d), the maximum temperature of HTS transformer coated by solid insulation, barely reaches 112 K for a 500 ms fault and could recover under full load. This means that not only the HTS transformer does not experience any burnouts or significant temperature rise but also could be used as fault tolerant transformer continuously delivers full load immediately after fault.

There is also another consideration about the recovery of YBCO tapes, known as partial recovery. The concept partial recovery is related to the part of the recovery that happens when temperature goes back from maximum temperature to close to the base temperature. Recovery has a much faster phase when conductor comes back from nucleate boiling regime to conduction/convection regime. In this regime, further cooling down and reaching to base temperature is dramatically slow and take hours. This concept is dedicated to the time duration that winding requires to completely return to base temperature. As shown in Figure 12, it takes a long time for YBCO tapes to return exactly to the base temperature, about 1 hour as reported in [5]. This is due to the fact that when temperature becomes lower than the critical temperature, the conduction/convection heat transfer took place. Under such heat transfer regime, a small amount of heat is transferred to cryogenic coolant fluid and former and as a result of this, the aforementioned recovery time becomes very long.

The next step is to analyze how much over-loading after 500 ms fault, could results in thermal runaway of the 50 MVA FTCL-HTS transformer with Acrylated Urethane solid insulation. Figure 13 indicates the time dependency temperature of FTCL-HTS transformer on secondary side while the loading is increased beyond 100%. As can be seen in this figure, even for 200% loading (100 MVA), the HTS transformer could recover safely, and therefore, survive without any damages to YBCO windings. However, the breaking point is about 225% loading (112.5 MAV) and by this loading, the YBCO tapes suffer a very quick thermal runaway and would be quickly burnt. This is due to the fact that by increasing the loading to be more than 225% of nominal load (i.e. 125% over-loading), film boiling heat transfer is occurred and as a result of this, YBCO tapes transit to thermal runaway mode.

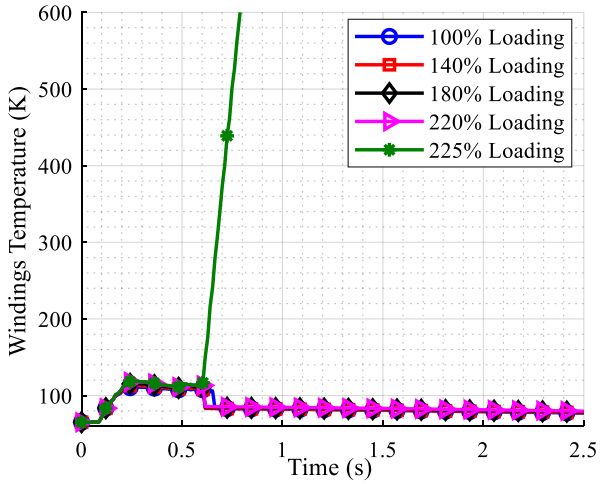

Figure 13. The impact of overloading on the recovery performance of a 50 MVA FTCL-HTS transformer with solid insulation

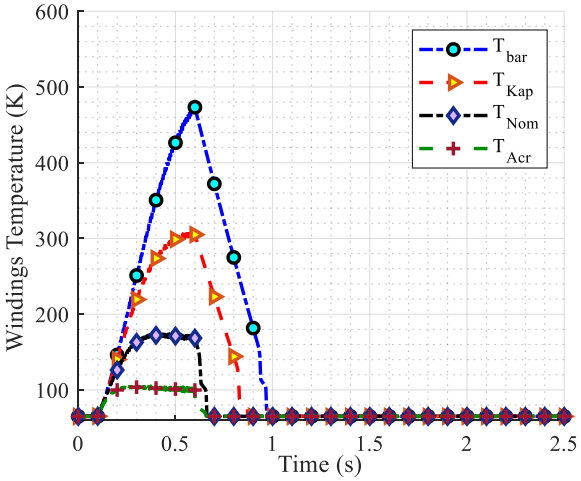

Figure 14. Free recovery process of different insulated tapes for a 500 ms fault

At last, free recovery of all types of superconducting tapes is shown in Figure 14. This figure shows the impact of insulation on the thermal behavior of FTCL-HTS transformer when no load is considered during recovery. This figure presents the impact of different heat-transfer coefficients on the final temperature and recovery time. In free recovery, it took for bare tape transformer around 400 ms to recover while this value for Kapton insulated tapes, Nomex insulated tapes, and Acrylated Urethane insulated tapes is around 200, 100, and 30 ms. The short recovery time of Acrylated Urethane insulated tapes is due to the low maximum temperature and high heat transfer. Table 6 tabulates the maximum loading value for each kind of tape after which HTS transformer could also recover.

2) Effect of fault duration on characteristics of FTCL-HTS transformer

The IEC 60076–5 standard requires all transformers to withstand against short circuit fault for 2 s, i.e. 2000 ms. The next step is to analyze the performance of 50 MVA FTCL-HTS transformer with Acrylated Urethane solid-insulated windings under longer duration faults. To do this, short circuit fault is applied to the transformer with 4 different durations, 0.5, 1, 1.5, and 2 s while the amplitude of all faults is around 20 times higher than nominal current. The aim is to analyze the

TABLE 6. Maximum recoverable loading after fault clearance for different insulations

Tape	Maximum loading for a recoverable fault (%)
Bare	50
Kapton insulated	55
Nomex insulated	65
Acrylated Urethane insulated	225

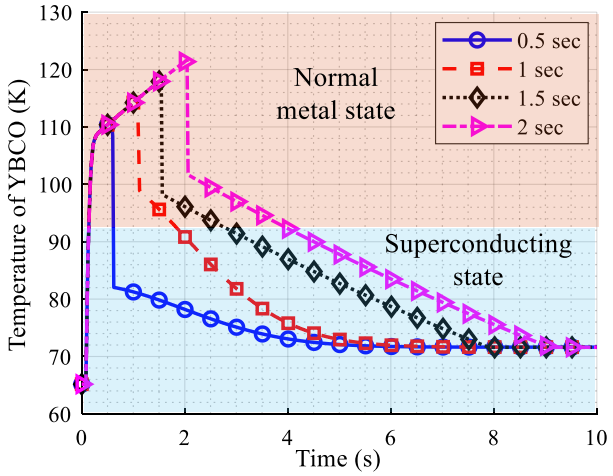

Figure 15. The impact of fault duration on the thermal characteristic of FTCL-HTS transformer with solid insulation under 100% loading after fault clearance

temperature increase rate and recovery under full loading of HTS transformer. The time dependency of temperature in secondary side windings of FTCL-HTS transformer is depicted in Figure 15. As it was expected, the longer fault causes maximum temperature to increase more. Also, the longer fault duration is, the transition to superconducting state occurs more lately after fault clearance, i.e. slower recovery. For 0.5 s fault, only 50 ms after fault clearance, HTS transformer transits to superconducting state while this value for 1, 1.5, and 2 s faults, are about 750 ms, 1300 ms, and 2100 ms, respectively. Also, a very long time is required for all fault duration to fully recover to base temperature (65 K) which is about more than half an hour. This is due to the fact that when temperature is reduced to lower than critical temperature of YBCO tapes, the heat transfer regime becomes natural convection. In this regime, a very low amount of heat is transferred and thus temperature is reduced very slowly. However, still this full load or over-load can be applied to the transformer. The important finding is that the HTS transformer could tolerate a three-phase fault for 2 s without burnout, or thermal runaway.

3) Fault current limiting capability of FTCL-HTS transformer

So far, we have discussed the fault tolerability of a 50 MVA HTS transformer, now the discussion must be made on fault current limiting capability of the HTS transformer. As shown in Figure 16, around 45 kA fault current is applied to the HTS transformer for 100 ms while the fault current is highly reduced

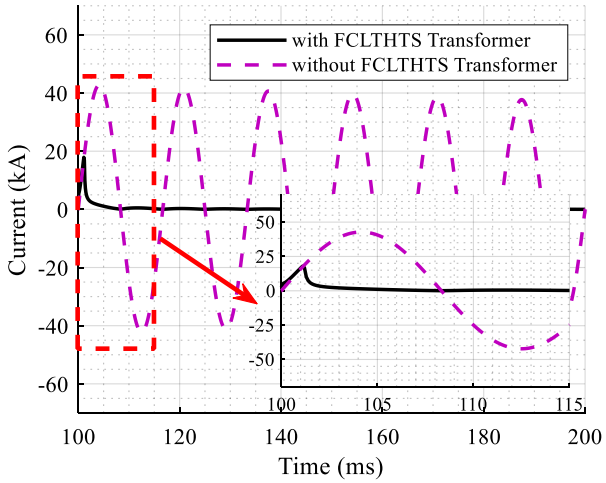

Figure 16. The fault current limiting performance of understudied HTS transformer

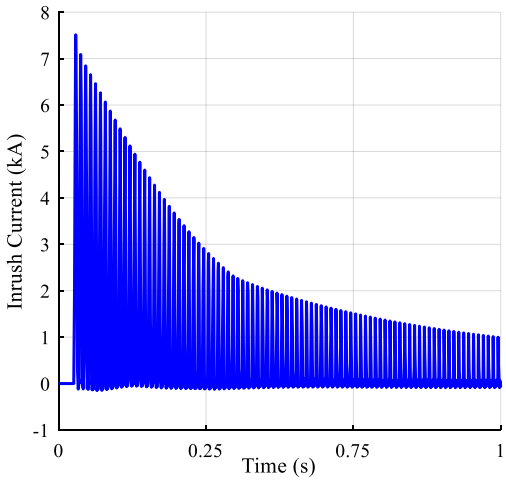

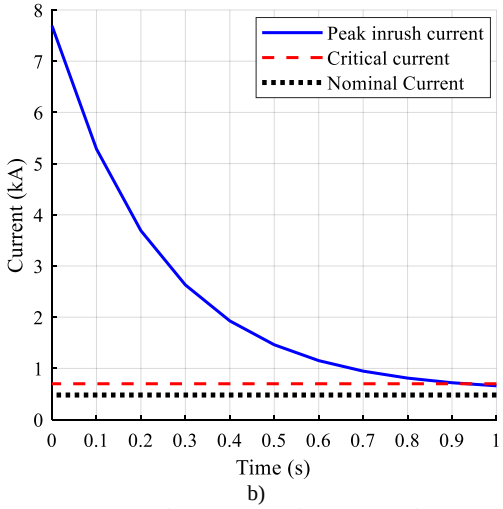

Figure 17. Inrush current of the HTS transformer under first energization in LN_2, a) Instantaneous inrush current, b) Peak of inrush currents versus time

and only a fraction of fault current passes through superconducting layer of YBCO tapes. This is due to the transition of HTS tapes to a non-superconducting state as a result of temperature increase. As results of resistivity increase, the fault current is dissipated in form of heat in superconducting transformer without possibility of thermal runaway or burnout.

Table 7. The thermal effect of inrush current with respect to different insulations

Insulation	Maximum Temperature (K)
Bare tape (non-insulated)	82.3
Kapton insulated	77.6
Nomex insulated	69.9
Solid insulation	67.5

By using solid insulation, the HTS transformer not only tolerate the fault for more than 2 seconds but also limits it to reduce the risk of failures and damages in other components of the power grid. Thus, the solid-insulated HTS transformer not only is fault-resistive but also operates as a component that protect the power system against faults.

C. The impact of Inrush current

The maximum value of the inrush current may increase to more than 10 times the value of the rated current [26], [27]. The amplitude of this current depends on factors such as the switching angle, the B-H characteristic of the core, the Thevenin impedance of the power system, the resistance of the primary winding, and the polarity of the residual magnetic flux density in the core at the switching moment. The energization of transformers causes a relatively high current passes through the windings that is known as inrush current. Instantaneous inrush current of this 50 MVA HTS transformer and its attenuation are shown in Figure 17(a) while peak values of inrush current along with nominal current and critical current are shown in Figure 17(b). After about 1 second the inrush current is fairly damped. As a result of the inrush current, temperature also increases. The maximum temperature of the HTS winding in LN_2 for different insulations are reported in Table 7. To gain the exact value, we had to calculate the inrush current by the presented equations and as can be seen, the value of calculated inrush current is relatively higher than nominal current. But what make the inrush current an important parameter, is the fact that it usually has a longer time duration than the short circuit faults. Fault durations are usually in milliseconds range (as protection relay system quickly isolate it) while inrush currents have duration in the range of seconds. Therefore, inrush currents impose a Lorentz force to the winding for much longer time while faults usually impose mechanical forces, such as Hoop stress for a very short time. It should be also noted that the value and duration of inrush current depends on many factors and can be changed. These factors are core structure, core type, X/R ratio of the grid, and many other factors.

In this study, B_{peak} is considered to be 1.6 T, B_{sat} is considered to be 2.2 T, and residual flux density for first time step is about 0.6 of the B_{peak} [17].

D. Using LH_2 as a method towards the FTCL-HTS transformer

In this subsection, the second strategy for having a FTCL-HTS transformer is discussed. Better heat transfer and faster recovery is the consequence of reducing the operational

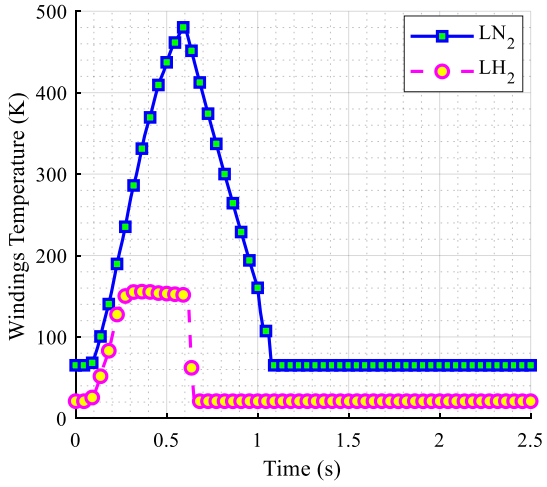

a)

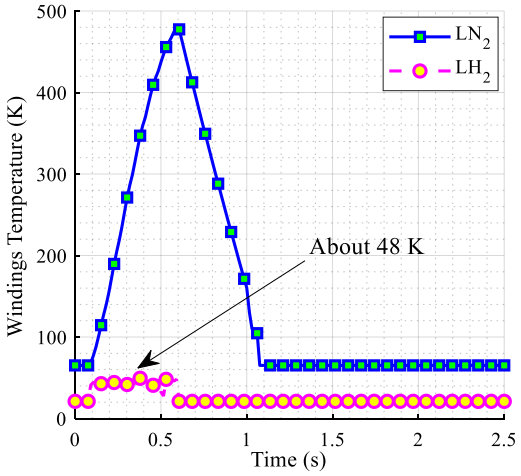

b)

Figure 18. Time dependency of temperature of secondary HTS winding of the FTCL-HTS transformer, a) Equal fault energy, b) Equal maximum fault current

temperature by changing the coolant from LN_2 to LH_2. LN_2 could not be used as cryogenic fluid in temperatures lower than 65 as nitrogen may get frozen. Meanwhile, LH_2 is considered as a promising coolant operating at 20 K for many new superconducting applications. When critical current is increased and temperature is changed from 65 K to 20 K, the design of HTS transformer would be completely different. We have tried to make a fair comparison between the performance of HTS transformers cooled down with LN2 and LH2 by making the input fault energy equal for both cases. To do so, we increased the fault current amplitude of HTS transformer with LH2 to make its fault energy equal to LN2-based transformer. However, a more detailed discussion about the fault performance, design, and power rating is the topic of our forthcoming studies.

The critical current of YBCO tapes used in this paper in 20 K is roughly 6 times higher than that of 65 K [28]. The fault current level of transformer with LH_2 is increased to reach around 120x higher than nominal current while this value of HTS transformer with LN_2 is about 20x. By doing this for a 500 ms

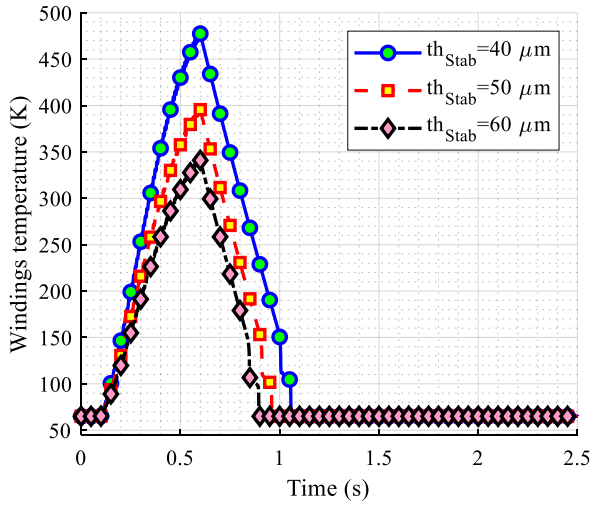

Figure 19. The impact of the stabilizer thickness on the thermal characteristic of 50 MVA HTS transformer

fault, an amount of energy about 1.4 MJ is imposed to the HTS winding. It should be mentioned that both results were accomplished for bare tapes with recovery under 10% of load after fault clearance. As a result of such a fault, the maximum temperature of HTS winding in LN_2 and LH_2 reaches to about 480 K and 160 K, respectively, as shown in Figure 18(a). Another scenario is also considered when the fault current levels are same and fault energies are different. In this scenario fault current level for both coolants is about 20 times higher than nominal current and this results in an unequal fault energy. Under such circumstances, LH_2 has still privilege in terms of maximum tolerable fault current, maximum temperature of Figure 18(b), and lower recovery time. Indeed, if one replaces LN_2 with LH_2, the transformer could operate as FTCL-HTS transformer. This is due to higher specific heat capacity of LH_2, higher value of heat flux during nucleate boiling state, and better heat transfer in 20 K, in comparison to LN_2 at 65 K.

E. The impact of stabilizer thickness on fault performance of HTS transformer

The third strategy for having a FTCL-HTS transformer is increasing the total heat capacity of the coated conductor tape of the winding. For this purpose, the thickness of stabilizer layer is increased from 40 µm to 60 µm. By doing this, the amount of thermal mass of YBCO tapes increases and thus more energy during fault is required to increase the temperature of tapes for 1 K. Although it is plausible that a larger stabilization thickness reduces the maximum temperature. But it is highly probable that it also reduces the current limiting capability of the transformer.

The results of Figure 19 show the windings temperature of HTS transformer for 500 ms fault current while just 10% of loading is applied after fault clearance. In this figure "th" stands for thickness of stabilizer layer. The maximum temperature of 40 µm stabilizer is around 20% higher than that of 50 µm scenario and this value for 60 µm scenario is about 37%. This shows that by increasing the thickness of stabilizer for even 10 µm, a large amount of heat capacity is added to the HTS transformer and could make it a FTCL-HTS transformer. Also, tape with 60 µm stabilizer recovers to superconducting state 40% faster than stabilizer with 40 µm thicknesses and this value for 50 µm stabilizer is 20%. Thus, not only stabilizer thickness impacts the maximum temperature of HTS transformer but also reduces the recovery time after fault clearance.

IV. Conclusion

The application of Fault Tolerant Current Limiting (FTCL) High Temperature Superconducting (HTS) transformers in power systems with a penetration level of wind farms could be beneficial due to their ability in supplying power during faults and reducing the level of fault current. Thus, in this paper, an equivalent circuit models (ECM) is developed for a 50 MVA 132/13.8 kV HTS transformer while experimental data are used to justify the simulation results. To make the HTS transformer fault tolerant, one strategy is presented by using three types of insulations, i.e. Kapton, Nomex, and Acrylated Urethane. Second strategy is analyzing the impact of Liquid hydrogen (LH_2) on the thermal characteristic of HTS transformer. At last, the impact of thermal capacity of stabilizer layer is analyzed on the fault tolerability of HTS transformer.

The most important findings of this paper are:

- The results of the proposed model are in a very good agreement with experimental results, as discussed in validation section.
- Among the proposed insulations, Acrylated Urethane has the best performance and for a 500 ms fault, the maximum temperature of windings covered with this insulation reaches 110 K while this value for bare tapes, Kapton insulated tapes, and Nomex insulated tapes is 480 K, 305 K, and 195 K, respectively.
- Acrylated Urethane insulated windings are capable of tolerating 2 s fault without any burnout or thermal runaway while the peak temperature is around 120 K.
- The FTCL-HTS transformer with Acrylated Urethane insulated windings reduces the fault current to 66% of the prospective fault current (with no FTCL-HTS transformer implemented in the grid).
- Acrylated Urethane insulated windings recover faster than other types of windings.
- By using liquid hydrogen as coolant for HTS transformer, maximum temperature of windings after a 500 ms fault is about 67% reduced, in comparison to the transformer that uses liquid nitrogen as coolant.
- By increasing the heat capacity of stabilizer, maximum temperature of HTS transformer under a 500 ms fault is about 20-40% reduced.

The proposed structure for HTS transformers has a high capability in limiting and tolerating fault currents and thus could be used as a solution for protecting power systems with wind farms or any other type of renewable energy resources.

As a future outlook, it must be noted that the performance of HTS transformers against fault currents, hot spots, and inrush currents could even further improved by implementation of artificial intelligence methods for windings optimal design, cryostat design, tape architecture design, and transformer protection [29].

REFERENCES

[1] M. P. Staines, Z. Jiang, N. Glasson, R. G. Buckley, and M. Pannu, "High-temperature superconducting (HTS) transformers for power grid applications," in *Superconductors in the Power Grid*, Woodhead Publishing, 2015, pp. 367–397.

[2] M. Mahamed, M. Yazdani-Asrami, V. Behjat, A. Yazdani, and M. Sharifzadeh, "Impact of Perlator on the Cooling Liquid Flow and Hottest Point Temperature of Superconducting Windings in HTS Transformer," *Superconductivity*, vol. 3, p. 100021, 2022.

[3] T. H. Han, S. C. Ko, and S. H. Lim, "Fault Current Limiting Characteristics of Transformer-Type Superconducting Fault Current Limiter Due to Winding Direction of Additional Circuit," *IEEE Trans. Appl. Supercond.*, vol. 28, no. 3, pp. 1–6, 2018, doi: 10.1109/TASC.2018.2793236.

[4] W. Song, Z. Jiang, M. Yazdani-Asrami, M. Staines, R. A. Badcock, and J. Fang, "Role of Flux Diverters in Reducing AC Loss in a Single-Phase 6.5 MVA HTS Traction Transformer for Chinese High-Speed Train Carrying High-Order Harmonic Currents," *IEEE Access*, vol. 10, pp. 69650–69658, 2022.

[5] M. Yazdani-asrami, M. Staines, G. Sidorov, and A. Eicher, "Heat transfer and recovery performance enhancement of metal and superconducting tapes under high current pulses for improving fault current-limiting behavior of HTS transformers," *Supercond. Sci. Technol.*, vol. 33, no. 9, p. 095014, 2020.

[6] M. Yazdani-Asrami *et al.*, "Fault current limiting HTS transformer with extended fault withstand time," *Supercond. Sci. Technol.*, vol. 32, no. 3, 2019, doi: 10.1088/1361-6668/aaf7a8.

[7] A. Sadeghi, S. M. Seyyedbarzegar, and M. Yazdani-Asrami, "Transient analysis of a 22.9 kV/2 kA HTS cable under short circuit using equivalent circuit model considering different fault parameters," *Phys. C Supercond. its Appl.*, vol. 589, no. July, p. 1353935, 2021, doi: 10.1016/j.physc.2021.1353935.

[8] J. Duron, F. Grilli, L. Antognazza, M. Decroux, B. Dutoit, and Ø. Fischer, "Finite-element modelling of YBCO fault current limiter with temperature dependent parameters," *Supercond. Sci. Technol.*, vol. 20, no. 4, p. 338, 2007.

[9] Y. Ichiki and H. Ohsaki, "Numerical analysis of AC losses in YBCO coated conductor in external magnetic field," *Phys. C Supercond. its Appl.*, vol. 412, pp. 1015–1020, 2004.

[10] Y. Yan, P. Song, W. Li, J. Sheng, and T. Qu, "Numerical Investigation of the Coupling Effect in CORC Cable with Striated Strands," *IEEE Trans. Appl. Supercond.*, vol. 30, no. 4, pp. 1–5, 2019.

[11] J. Wang, A. F. Witulski, J. L. Vollin, T. K. Phelps, and G. I. Cardwell., "Derivation, Calculation and Measurement of Parameters for a Multi-Winding Transformer Electrical Model," in *APEC '99. Fourteenth Annual Applied Power Electronics Conference and Exposition. 1999 Conference Proceedings*, 1999, pp. 220–226.

[12] A. Lapthorn, P. Bodger, and W. Enright, "A 15-kVA High-Temperature Superconducting Partial-Core Transformer - Part 1 : Transformer Modeling," *IEEE Trans. Power Deliv.*, vol. 28, no. 1, pp. 245–252, 2012.

[13] E. P. Volkov, E. A. Dzhafarov, L. S. Fleishman, V. S. Vysotsky, and V. V. Sukonkin, "First 1 MVA and 10/0.4 kV HTSC transformer in Russia," *Therm. Eng.* , vol. 63, no. 13, pp. 909–916, 2016, doi: 10.1134/S0040601516130085.

[14] M. Yazdani-Asrami, S. A. Gholamian, S. M. Mirimani, and J. Adabi, "Influence of Field-Dependent Critical Current on Harmonic AC Loss Analysis in HTS Coils for Superconducting Transformers Supplying Non-Linear Loads," *Cryogenics (Guildf).*, vol. 113, p. 103234, 2020.

[15] A. Morandi, L. Trevisani, P. L. Ribani, M. Fabbri, L. Martini, and M. Bocchi, "Superconducting transformers: Key design aspects for power applications," *J. Phys. Conf. Ser.*, vol. 97, no. 1, 2008, doi: 10.1088/1742-6596/97/1/012318.

[16] G. Komarzyniec, "Calculating the inrush current of superconducting transformers," *Energies*, vol. 14, no. 20, p. 6714, 2021, doi: 10.3390/en14206714.

[17] M. A. A. Rahman, T. T. Lie, and K. Prasad, "The Effects of Short-Circuit and Inrush Currents on HTS Transformer Windings," *IEEE Trans. Appl. Supercond.*, vol. 22, no. 2, pp. 5500108–5500108, 2012.

[18] B. Xiang *et al.*, "Study on the influencing factors to reduce the recovery time of superconducting tapes and coils for the DC superconducting fault current limiter applications," *High Volt.*, vol. 7, no. 3, pp. 483–495, 2021, doi: 10.1049/hve2.12158.

[19] M. Staines, M. Yazdani-Asrami, N. Glasson, N. Allpress, L. Jolliffe, and E. Pardo, "Cooling systems for HTS transformers: impact of cost, overload, and fault current performance expectations," in *," In 2nd International Workshop on Cooling Systems for HTS Applications (IWC-HTS)*, 2017, pp. 13–15.

[20] M. Yazdani-Asrami, M. Staines, and G. Sidorov, "Heat transfer in HTS transformer and current limiter windings," in *Proc. 2nd Int. Workshop Cooling Syst. HTS Appl.(IWC-HTS)*, 2017, pp. 4–5.

[21] T. Yasui *et al.*, "Temperature and Pressure Distribution Simulations of 3-km-Long High-Temperature Superconducting Power Cable System with Fault Current for 66-kV-Class Transmission Lines," *IEEE Trans. Appl. Supercond.*, vol. 27, no. 4, 2017, doi: 10.1109/TASC.2017.2656631.

[22] M. Podlaski *et al.*, "Multi-Domain Modeling and Simulation of High Temperature Superconducting Transmission Lines under Short Circuit Fault Conditions," *IEEE Trans. Transp. Electrif.*, vol. 8, no. 3, pp. 3859–3869, 2022, doi: 10.1109/TTE.2021.3131271.

[23] A. Sadeghi and S. meysam Seyyedbarzegar, "An accurate model of the high-temperature superconducting cable by using stochastic methods," *Transformers Magazine*, pp. 70–76, 2021.

[24] S. S. Kalsi, *APPLICATIONS OF HIGH TEMPERATURE SUPERCONDUCTORS TO ELECTRIC POWER EQUIPMENT*. John Wiley & Sons, 2011.

[25] M. Yazdani-Asrami, S. M. Seyyedbarzegar, M. Zhang, and W. Yuan, "Insulation Materials and Systems for Superconducting Powertrain Devices in Future Cryo-Electrified Aircraft: Part I—Material Challenges and Specifications, and Device-Level Application," *IEEE Electr. Insul. Mag.*, vol. 38, no. 2, pp. 23–36, 2022.

[26] M. Yazdani-Asrami, M. Taghipour-Gorjikolaie, S. M. Razavi, and S. A. Gholamian, "A novel intelligent protection system for power transformers considering possible electrical faults, inrush current, CT saturation and over-excitation," *Int. J. Electr. Power Energy Syst.*, vol. 64, pp. 1129–1140, 2015.

[27] M. Taghipour, A. R. Moradi, and M. Yazdani-Asrami, "Identification of magnetizing inrush current in power transformers using GSA trained ANN for educational purposes," in *2010 IEEE Conference on Open Systems (ICOS 2010)*, 2010, pp. 23–27.

[28] "Robinson HTS Wire Critical Current Data Base." https://htsdb.wimbush.eu/

[29] M. Yazdani-asrami, M. Taghipour-gorjikolaie, W. Song, M. Zhang, S. Chakraborty, and W. Yuan, "Artificial intelligence for superconducting transformers," *Transform. Mag.*, vol. 8, no. S5, pp. 22–30, 2021.